

# Rego: A Robust and Explainable Query Optimization Cost Model

Baoming Chang  
University of Ottawa  
Ottawa, Canada  
bchan081@uottawa.ca

Amin Kamali  
University of Ottawa  
Ottawa, Canada  
skama043@uottawa.ca

Verena Kantere  
University of Ottawa  
Ottawa, Canada  
vkantere@uottawa.ca

## ABSTRACT

In recent years, there has been a growing interest in using machine learning (ML) in query optimization to select more efficient plans. Existing learning-based query optimizers use certain model architectures to convert tree-structured query plans into representations suitable for downstream ML tasks. As the design of these architectures significantly impacts cost estimation, we propose a tree model architecture based on Bidirectional Graph Neural Networks (Bi-GNN) aggregated by Gated Recurrent Units (GRUs) to achieve more accurate cost estimates. The inherent uncertainty of data and model parameters also leads to inaccurate cost estimates, resulting in suboptimal plans and less robust query performance. To address this, we implement a novel learning-to-rank cost model that effectively quantifies the uncertainty in cost estimates using approximate probabilistic ML. This model adaptively integrates quantified uncertainty with estimated costs and learns from comparing pairwise plans, achieving more robust performance. In addition, we propose the first explainability technique specifically designed for learning-based cost models. This technique explains the contribution of any subgraphs in the query plan to the final predicted cost, which can be integrated and trained with any learning-based cost model to significantly boost the model’s explainability. By incorporating these innovations, we propose a cost model for a Robust and Explainable Query Optimizer, Rego, that improves the accuracy, robustness, and explainability of cost estimation, outperforming state-of-the-art approaches in all three dimensions.

### PVLDB Reference Format:

Baoming Chang, Amin Kamali, and Verena Kantere. Rego: A Robust and Explainable Query Optimization Cost Model. PVLDB, 18(1): XXX-XXX, 2025.

doi:XX.XX/XXX.XX

### PVLDB Artifact Availability:

The source code, data, and/or other artifacts have been made available at <https://github.com/BaomingChang/Rego-on-PostgreSQL>.

## 1 INTRODUCTION

Query optimization is crucial for database management systems (DBMSs), directly impacting query execution performance. Accurately and efficiently estimating the cost of candidate query execution plans and selecting the optimal one remains a significant challenge. A query execution plan is typically represented as a tree,

This work is licensed under the Creative Commons BY-NC-ND 4.0 International License. Visit <https://creativecommons.org/licenses/by-nc-nd/4.0/> to view a copy of this license. For any use beyond those covered by this license, obtain permission by emailing [info@vldb.org](mailto:info@vldb.org). Copyright is held by the owner/author(s). Publication rights licensed to the VLDB Endowment.

Proceedings of the VLDB Endowment, Vol. 18, No. 1 ISSN 2150-8097.

doi:XX.XX/XXX.XX

where nodes contain information about operators for accessing, joining, or aggregating data, and edges represent dependencies between parent and child nodes. An optimal plan allows the system to handle data efficiently. Traditional query optimizers use cost models based on statistical methods like histograms [10], which often introduce errors due to their limitations in capturing complex characteristics, such as join-crossing correlations. ML offers promising solutions for enhancing query optimization. Recent learning-based optimizers follow a common architecture (Figure 1), encoding node-level information into features that are then aggregated into a graph-level representation for each candidate plan. A cost estimator predicts execution costs based on these representations, enabling the optimizer to select the most efficient plan. However, preserving both node-level features and structural information between nodes when transforming tree-structured plans into representations is challenging, and any omission of key structural or operator details can diminish the effectiveness of downstream optimization.

Furthermore, due to ML models’ “black box” nature [18], the underlying rationale behind the predictions of learning-based cost models remains difficult for humans to understand and trust. Current approaches often overlook the explainability of these models, meaning that while they theoretically aggregate plan node features and structural information to generate representation and estimated cost, it remains unclear how specific subgraphs or operations within the query plan impact these predictions. Consequently, the lack of transparency on how specific plan components influence outcomes limits its effectiveness in trust-critical real-world applications.

Additionally, plan selection usually relies on the ranking of the cost model’s estimated costs for all candidate query plans. Due to inherent uncertainty, the plan selected by the query optimizer may not have the shortest execution runtime. Query optimization methods that are less sensitive to such estimation errors and do not rely on simplifying assumptions are considered robust [12], which is a critical avenue for improving the overall performance of the optimizer. Recent learning-based cost models have increasingly addressed robustness. Some approaches [3, 23, 24] implement it by

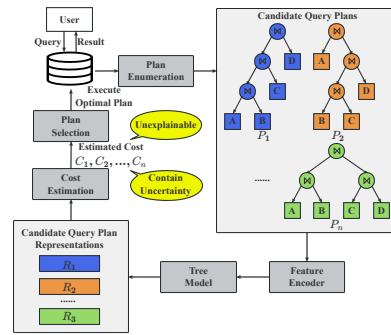


Figure 1: Basic learning-based query optimizer framework

mitigating misestimation of the input parameters or minimizing the possibility of selecting a worse plan through specific mechanisms. However, the state-of-the-art approaches [4, 5, 12, 19, 41] change to quantify the uncertainty in data and model predictions, applying such measures to improve the robustness of query optimization. These methods usually use approximate probabilistic ML to quantify uncertainties and apply them for more robust plan selection. Despite their superior performance, these models’ training (including cost and uncertainty estimation) remains decoupled from its plan selection strategy, limiting uncertainty exploitation and self-improvement through selection feedback.

In this paper, we focus on improving these challenges: query plan representation, cost estimation explainability, and plan selection robustness. Comparative studies on tree models [2, 44] highlight their critical role in query plan representation. Therefore, we propose a novel tree model architecture BiGG [2] that leverages Bi-GNNs [32] and a GRU-based aggregator [1]. This approach captures both node and structural information in query plan trees more effectively, providing superior representation learning capabilities compared to other advanced tree models [27, 36]. Additionally, we propose the first explainability technique for learning-based cost models that captures subtree-level contributions by quantifying similarities in subtree-plan representations. This approach pinpoints high-impact subgraphs that significantly influence execution cost, thereby enhancing transparency and improving trust in cost-based decisions. By identifying these critical subgraphs, developers can focus manual optimization efforts and increase efficiency in the query optimization process. To enhance robustness, we introduce a learning-to-rank cost model with uncertainty quantification. This approach adaptively integrates cost estimates and uncertainty for plan selection, benefiting from pairwise plan comparisons during training without requiring pairwise inputs at test time. As a result, it achieves considerable improvements in plan selection robustness.

To summarize, our main contributions are:

- We propose a novel, more powerful query plan tree model based on our previous work BiGG [2] with Bidirectional GNNs and a GRU-based aggregator.
- We introduce explainability into learning-based cost models for the first time by quantifying how query plan subgraphs affect cost estimation. This approach fosters transparency, provides a basis for targeted optimizations, and increases trust in the learning-based cost model’s predictions.
- We design and implement an uncertainty-aware cost model that employs a learning-to-rank mechanism capable of adaptively integrating the qualified cost estimation and uncertainty for query plan comparison while significantly improving the robustness of the model.
- We develop Reqo, a comprehensive query optimization cost model that integrates our three proposed techniques, and experimentally show its significant improvements in cost estimation accuracy, robustness, and explainability over state-of-the-art cost models.

In the rest of the paper: Section 2 outlines the problem statement, Section 3 details the three key techniques of Reqo, Section 4 presents Reqo’s architecture, Section 5 presents the experimental study, Section 6 reviews related work, and Section 7 concludes.

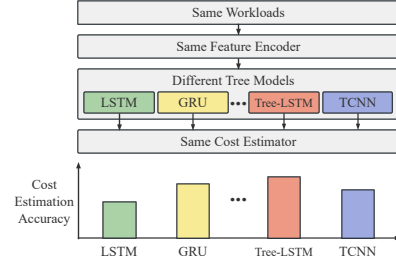


**Figure 2: Comparison of different tree models (such as LSTM, GRU, Tree-LSTM, TCNN) and their impact on cost estimation performance under the same workload and configurations**

## 2 PROBLEM STATEMENT

This section highlights three core challenges in learning-based query optimization. First, we discuss query plan representation, which demands accurately encoding tree-structured plans into vectors while preserving node-level and structural information. Second, we present the explainability gap arising from ML versus traditional cost models. Finally, we highlight the need for robustness against execution uncertainties and discuss the limitations of current uncertainty quantification practices. In the following, we detail each challenge and define the problems to be solved.

### 2.1 Query Plan Representation

In learning-based query optimizers, query plan representation learning begins with taking the physical query plan as input, using a feature encoder and tree model to generate plan representations. These representations encapsulate critical information, including operators, parent-child relationships, and underlying data, serving as essential inputs for downstream tasks. Consequently, their quality sets a performance ceiling for the entire cost model, making the tree model’s output pivotal to the optimization process.

**Example 2.1.** Figure 2 shows a comparative study on tree models [2], showing that different tree models yields varying cost estimation performance under identical workloads and optimizer configurations, which highlights the importance of tree models. □

Formally, a physical query plan is represented as a rooted tree  $T = (V, E)$ , where each node  $v \in V$  represents an operator and edges  $(v', v) \in E$  specify child-to-parent relationships, defining execution dependencies from leaves to the root. Each node  $v$  has a feature vector  $\mathbf{x}_v \in \mathbb{R}^d$ , capturing node-level information such as operators, relations, and predicates. The objective is to design a tree model  $g_\phi$ , parameterized by  $\theta$ , that maps the tree  $T$  and the node features  $\{\mathbf{x}_v\}_{v \in V}$  to a fixed-size representation  $\mathbf{h}_T \in \mathbb{R}^k$ :

$$\mathbf{h}_T = g_\phi(T, \{\mathbf{x}_v\}). \quad (1)$$

A downstream model  $f_\theta$ , parameterized by  $\phi$ , utilizes this representation to predict the estimated execution cost  $\hat{y} \in \mathbb{R}$ :

$$\hat{y} = f_\theta(\mathbf{h}_T). \quad (2)$$

The optimal  $\theta^*$  and  $\phi^*$  are obtained by minimizing the expected cost estimation error over the distribution of query plans  $\mathcal{D}$ :

$$\theta^*, \phi^* = \arg \min_{\theta, \phi} \mathbb{E}_{(T, \{\mathbf{x}_v\}, y) \sim \mathcal{D}} \left[ \mathcal{L} \left( f_\theta \left( g_\phi(T, \{\mathbf{x}_v\}) \right), y \right) \right], \quad (3)$$

where  $\mathcal{L}$  is a loss function and  $y$  is the actual execution cost.

The key challenge lies in devising a tree model  $g_\phi$  that accurately captures both node-level features (e.g., operators, relations, and predicates) and their structural dependencies. Effectively preserving these details minimizes information loss, allowing the downstream model  $f_\theta$  to reliably assess the impact of each node and its position in the hierarchy on the overall execution cost. As a result, improving the tree model directly enhances the quality of the query plan representation and drives more accurate cost estimation. By bolstering  $g_\phi$ 's ability to encode complex query plans, learning-based query optimizers can achieve superior performance in downstream tasks and more efficient database management.

## 2.2 Explainability of Learning-based Cost Model

In classical query optimizers, cost models typically rely on statistical methods (e.g., histograms) and use a transparent, modular structure. The total cost of a query plan is the sum of its constituent operators' or subplans' costs. In such models, for a query plan tree  $T$ , the cost of a parent node  $v_p$  derives from its children's costs plus a local cost capturing the operator's own overhead:

$$C_{\text{classical}}(v_p) = c(v_p) + \sum_{v_c \in \text{children}(v_p)} C_{\text{classical}}(v_c) \quad (4)$$

where  $c(v_p)$  is a function that estimates the local cost of operator  $v_p$ . By recursively applying Eq.4 from the leaves to the root of the query plan, the total estimated cost of  $T$  is obtained as:

$$C_{\text{classical}}(T) = C_{\text{classical}}(\text{root}(T)) \quad (5)$$

This bottom-up aggregation makes final estimates clearly traceable to each node, enabling developers to tune performance at the operator or subplan level with clear insights into how local costs flow into the final total cost. In contrast, learning-based cost models predict the cost  $C_{\text{learned}}(T)$  using a parameterized (often black-box) function  $f_\theta$  trained on historical query data, which do not explicitly decompose the plan into subgraphs in an interpretable way. Although these models often yield higher accuracy, they forgo the built-in transparency of classical approaches and obscure how individual predicates or local substructures affect the total estimate. This lack of transparency hinders the diagnosis of cost misestimations, complicates fine-grained tuning, and erodes trust when estimates deviate from observed execution times.

To restore the beneficial transparency of classical cost models, a learned cost model should have the ability to quantify the contribution of each subgraph  $G_s \subseteq T$  to the total cost  $C_{\text{learned}}(T)$ . These subgraphs typically correspond to logical or physical subplans that can be individually optimized (e.g., specific joins or indexes). Identifying their contributions helps developers locate bottlenecks or highlight operators that may benefit from tuning or rewriting.

*Definition 2.1 (Explainability of a Learning-based Cost Model).* Let  $G_s = (V_s, E_s)$  be any subgraph of  $T = (V, E)$ , with  $V_s \subseteq V$  and  $E_s \subseteq E$ . A model is considered to have explainability with respect to subgraph contributions if there exists a function:

$$F: \{(G_s) \mid G_s \subseteq T\} \rightarrow \mathbb{R} \quad (6)$$

that quantifies how  $G_s$  influences  $C_{\text{learned}}(T)$ . Since a black-box model  $f_\theta$  does not directly expose how individual subgraphs contribute to the overall cost,  $F$  must be derived or learned to capture

the contribution at the subgraph level and maintain enough fidelity for optimizing subplans and identifying bottlenecks.

The goal of explainability is to accurately quantify each subgraph's actual contribution to the total cost in a learning-based query optimizer. Formally, we seek the function  $F^*$  that estimates the contribution with minimal error:

$$F^* = \arg \min_F \text{ExplanationLoss}(F(G_s), \hat{F}(G_s)), \forall G_s \subseteq T \quad (7)$$

where  $\text{ExplanationLoss}$  captures the difference between the subgraph's actual contribution (approximated by  $\hat{F}$ ) to the overall cost and the contribution estimated by  $F$ . Reducing  $\text{ExplanationLoss}$  ensures that each subgraph-level explanation is faithful to actual query execution, thereby restoring the transparency of classical models and providing a basis for fine-grained performance tuning.

## 2.3 Robust Learning-based Cost Estimation

Most cost models prioritize the accuracy of cost estimates in their design, often overlooking inherent uncertainties. In reality, uncertainties in query plan execution are significantly influenced by factors such as structural characteristics, specific operations or predicates, and data properties. Moreover, estimation methods themselves may introduce further limitations. In this context, robustness in cost estimation refers to the ability of a cost model to maintain accurate plan selection despite these inherent uncertainties.

The classical problem of optimal plan selection is defined as: given a finite set of candidate execution plans  $\mathcal{P} = \{p_1, p_2, \dots, p_n\}$  and a cost function  $f(p_i)$  that estimates the cost of executing plan  $p_i$  for  $i = 1, \dots, n$ , the goal is to find the optimal plan  $p^*$  such that:

$$p^* = \arg \min_{p_i \in \mathcal{P}} f(p_i) \quad (8)$$

This formulation overlooks the inherent inaccuracies in estimated costs, which may lead to selecting suboptimal plans at runtime. Robust query optimization aims to minimize such risks by incorporating uncertainties. Here, we introduce a function  $u(p_i)$  that quantifies the uncertainty in the cost estimate for plan  $p_i$ . The robust plan selection problem is then formulated as finding the plan  $p^*$  that considers both estimated cost and uncertainty:

$$p^* = \arg \min_{p_i \in \mathcal{P}} h(f(p_i), u(p_i)) \quad (9)$$

where  $h$  is a function representing the optimizer's strategy in balancing cost and uncertainty.

A key challenge is quantifying these uncertainties and incorporating them into query optimization to achieve more robust performance. Current state-of-the-art research quantifies model uncertainty through methods such as Bayesian neural networks [34], Monte Carlo Dropout [11]; Gaussian negative log-likelihood [28] and spectral-normalized neural Gaussian processes [20] for query plan data uncertainty. After computing  $u(p_i)$ , they use predefined rules in plan selection to balance  $f(p_i)$  and  $u(p_i)$ , thereby finding more robust and efficient plans. However, a significant limitation is that plan comparisons are excluded from the cost model's training, preventing adaptive refinement of its balancing strategies.

In summary, designing an adaptive balancer  $h$  that reconciles  $f(p_i)$  and  $u(p_i)$  while incorporating plan comparison results into the cost model's training remains a critical challenge for enhancing the robustness of learning-based query optimization.

### 3 MODEL OVERVIEW

Addressing the three main challenges from Section 2: limited query plan representation expressiveness, lack of explainability in cost estimations, and the need for robust plan selection under uncertainty, we propose an integrated solution consisting of three techniques. First, we introduce BiGG (Section 3.1), a novel representation learning method based on bidirectional GNNs and GRU, which preserves both node-level features and structural information, producing higher-quality plan representations. Second, to tackle the black-box nature of learned cost models, we develop a subtree-based explainability technique (Section 3.2) that quantifies the contribution of query plan subgraphs to cost predictions, restoring transparency comparable to classical methods while achieving higher accuracy. Finally, we present a robust learning-to-rank cost model (Section 3.3) that adaptively quantifies and integrates uncertainty into the plan selection process via pairwise plan comparisons, mitigating suboptimal choices arising from estimation errors or volatile execution environments. In the following, we detail each technique and illustrate how it addresses its corresponding challenge.

#### 3.1 BiGG: A Novel Technique for Query Plan Representation Learning Based on Bi-GNNs

To improve query plan representation, we build on our previous work [2] by introducing BiGG, a novel representation learning method that leverages bidirectional GNNs and a GRU-based aggregator. This design preserves more during transformation, produces higher-quality plan embeddings, and yields more precise cost predictions, providing a robust foundation for downstream tasks.

**3.1.1 Bidirectional GNNs.** To improve the tree model’s ability to represent query plans accurately, we employ GNNs due to their proficiency in capturing graph topology [14]. We innovatively treat the query plan trees as two single-directional graphs with opposite edge directions (parent-to-child and child-to-parent). In each layer (Figure 3), these two graphs are processed independently by TransformerConv [33] layers. We then integrate the corresponding node features from the two output learned graphs through a learnable parameter, which makes it possible to transmit information in both directions while still utilizing the direction information of the edges and retaining relevant structural information. This bidirectional GNN design facilitates information flow in both directions, enabling nodes to learn from both sides, unlike using single-directional edges. By treating the query plan tree as two graphs with opposite edge directions, the model preserves dependencies between parent and child nodes compared to using undirected edges. TransformerConv layers with multi-head attention [37] allow each node to adaptively aggregate neighbour information, enhancing the model’s ability to capture the tree’s local graph topology and global dependencies. This design benefits from GNNs but addresses the limitations of single-directional and undirected GNNs in learning query plans, markedly improving tree-structured plan representation learning.

**3.1.2 Aggregation Operator based on GRUs.** Conventional graph aggregation methods often yield suboptimal results with query plans because they typically use global pooling of node features, ignoring the tree’s structural information. To address this, we apply

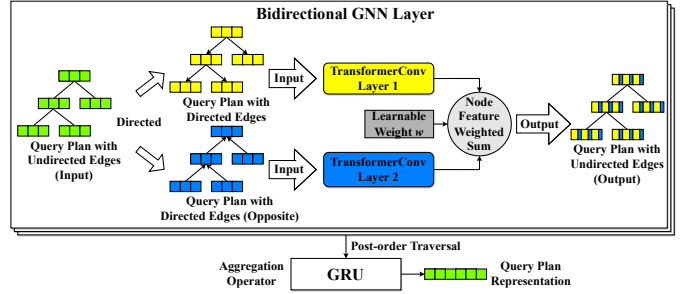


Figure 3: The architecture of BiGG using bidirectional GNN with a GRU-based aggregator

a GRU [1] to aggregate the GNN-derived node features after post-order traversal of the tree. This ordering aligns with how DBMSs execute plan nodes [21], allowing the model to selectively retain or forget features and learn how the operation order affects the cost. Consequently, we can capture node dependencies more accurately and closely align with the actual execution sequence, enabling BiGG to obtain the query plan’s graph-level embedding while retaining essential node and structural information.

**3.1.3 Stronger Basis for Downstream Techniques.** By capturing both node-level features and structural dependencies, BiGG serves as a powerful instantiation of  $g_\phi$ , effectively addressing the representation problem outlined in Section 2. The richer representation not only enhances  $f_\theta$ ’s cost estimation accuracy but also provides a stronger foundation for our subsequent techniques: Specifically, our subtree-based explainer (See Section 3.2) can more precisely assess each subplan’s contribution to overall cost based on their embeddings, thus elucidating how particular subgraphs drive execution time; Additionally, our robust learning-to-rank cost model (See Section 3.3) benefits from these enhanced embeddings to better distinguish subtle plan differences under uncertainty, mitigating misestimation risks and leading to more reliable plan selection.

#### 3.2 An Explainability Technique for Learning-based Cost Models

In Section 2.2, we discuss the lack of transparency in learning-based cost estimators. To address it, we propose a novel subtree-based explainability technique that extracts valid subtrees from a query plan, ensuring each subplan remains executable and retaining all essential operators and relations for accurate contribution estimation. We then employ a learning-based method to quantify the embedding similarity between each subtree and the full plan. This similarity measure allows the model to automatically learn and infer how each subgraph influences the final cost prediction, restoring transparency similar to traditional cost models. Below, we explain how to extract these subtrees, measure their embedding similarity, and integrate these insights into a learning-based explanation technique that trains simultaneously with the cost model.

**3.2.1 Subgraph Extraction Based on Query Plan Subtrees.** To explain the impact of subgraphs on the final cost prediction of query plans, a straightforward approach is to feed each subgraph  $G_s$  directly into the cost model. However, query plan trees impose strict parent-child dependencies, and omitting any child node creates

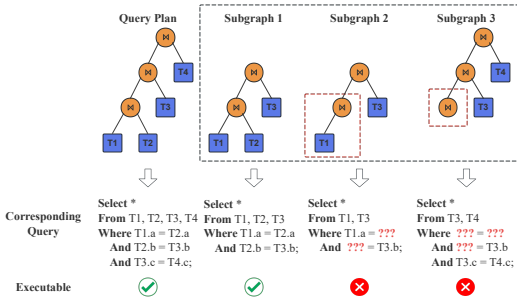


**Figure 4: Incomplete child nodes extraction in the query plan results in unexecutable subplans**

incomplete subplans that lack essential relational and operational details, producing unexecutable plans and unreliable estimates.

**Example 3.2.** Subgraphs 2 and 3 in Figure 4 illustrate this issue. Since the scan operations on tables T1 and T2 are omitted, the cost model can not estimate the join operation properly, yielding unexecutable subplans. □

To avoid losing key nodes during subgraph extraction, we introduce a subtree-based approach. Specifically, we segment the query plan into subtrees, each rooted at a chosen node and extending down to all its leaf nodes. As depicted in the upper half of Figure 6, the process begins with individual leaves and expands to larger subtrees until the entire plan is covered. DBMSs such as PostgreSQL record the cumulative execution time (i.e., Total actual time) of each node along with all its child nodes. Consequently, for any complete subtree, the execution time recorded at its root node directly reflects the subtree’s actual runtime, serving as a training label that denotes its contribution to the overall query plan cost.

**3.2.2 Similarity Quantification Between Query Plan and Subtree Embeddings.** We propose an approach to estimate the impact of subtrees on cost predictions by quantifying the embedding similarity between query plans and their subtrees. The literature [22] shows that if a subgraph significantly impacts the final prediction, there should be a notable similarity between the subgraph’s embedding and the complete graph’s embedding, enabling the model to make similar decisions. The similarity can be measured using functions such as cosine similarity, mutual information (MI) [15] and learning-based methods. By ranking these similarities, the subgraphs with the greatest impact on predictions can be identified.

**Example 3.3.** Figure 5 shows a query plan tree where each node displays the model’s estimated execution time for its subplan. We extracted several subplans to explore the relationship between the cosine similarity of subplan embeddings to the complete plan embedding and their influence on the final prediction. The contribution is defined as the ratio of the subplan’s execution time to that of the complete plan. For example, subplan 1, although just a leaf, has the highest cosine similarity (0.754) and the largest contribution (0.768). In contrast, subplan 2 shows low similarity (0.120) and minimal contribution (0.005). Subplans 3 and 4 exhibit moderate similarity and contribution. These observations indicate a positive correlation between embedding similarity and subplan contribution. □

Hence, measuring the similarity between a subtree and the entire query plan can reflect that subtree’s contribution to the total cost. By employing a learning-based model to adaptively quantify

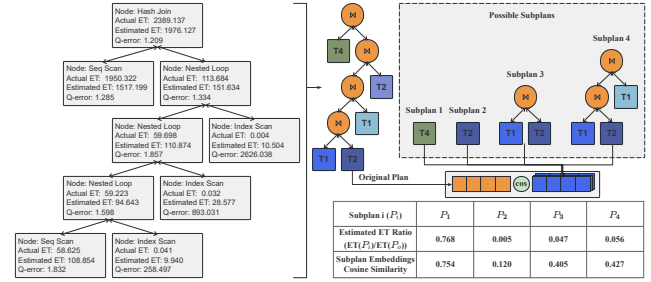


**Figure 5: Example of the relationship between the cosine similarity of the overall query plan and subplan embeddings, and their influence on the cost prediction result**

this similarity, we can instantiate  $F$  in Section 2.2. Aligning each subgraph’s embedding with the overall plan embedding allows the model to assess the subtree’s impact on the learned cost estimate as shown in Figure 6, thus explaining the relations between black-box predictions  $C_{\text{learned}}(T)$  and local subgraphs  $G_S$ , providing the explainability function to learning-based cost models.

**3.2.3 Learning-based Explainability Technique.** Building on subtree extraction and subtree–plan embedding similarity, we propose an explainability technique for learning-based cost models, as shown in Figure 6. We first extract subtrees of various sizes from the original query plan and encode them (along with the full plan) using the same tree model  $g_\phi$ . During training, a learning-based explainer model  $\Psi$  automatically learns the contribution of each subtree to the overall cost prediction. In particular,  $\Psi$  estimates the contribution  $EC_{st_k} \in [0, 1]$  of each subtree  $k$  by quantifying the similarity between its embedding  $\text{Emb}_{st_k}$  and the embedding of the complete query plan  $\text{Emb}_{ot}$  as below:

$$EC_{st_k} = \Psi(\text{CONCAT}(\text{Emb}_{st_k}, \text{Emb}_{ot})), EC_{st_k} \in [0, 1] \quad (10)$$

The actual contribution ratio  $AC_{st_k}$  is defined as the ratio of the subtree’s actual execution time to entire plan’s total execution time:

$$AC_{st_k} = \frac{ET_{st_k}}{ET_{ot}}, AC_{st_k} \in [0, 1] \quad (11)$$

where the actual contribution ratio of the original query plan tree is always 1. An explanation loss function is designed to minimize the discrepancy between the estimated and actual contribution ratios: Given a query plan set  $P$  with  $N$  plans, a plan  $p_i$  with  $K_i$  subtrees where  $p_i \in P$ , the explanation loss is shown as:

$$\text{ExplanationLoss} = \frac{1}{N} \sum_{i=1}^N \left( \frac{\sum_{k=1}^{K_i} (AC_{st_{ik}} - EC_{st_{ik}})^2}{K_i} \right) \quad (12)$$

Thus, the explainer learns the relationship between subtree embeddings and the complete plan embedding, enabling it to estimate contribution ratios and explain the cost model’s predictions. After training, for cost estimations that do not require explanations,  $\text{Emb}_{ot}$  can directly represent the query plan without extracting subtrees or activating the explainer, reducing inference time. When explanations are required, the technique estimates each subtree’s contribution, revealing how every subgraph or node operation affects the final prediction, as outlined in Algorithm 1.

This explainability technique addresses the challenge in Section 2.2. We employ the learning-based explainer as the function

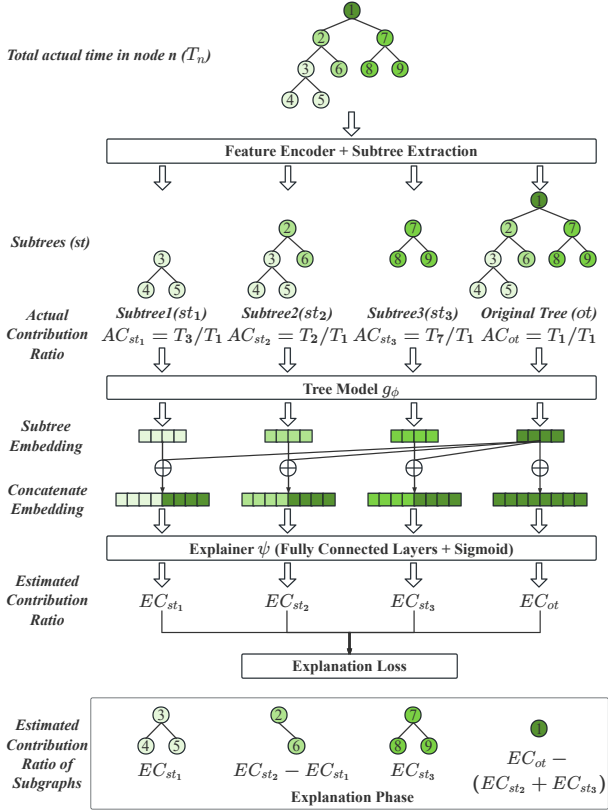


**Figure 6: The explainability technique for query plan cost model based on query plan subtrees**

$F$  to quantify subplan contributions,  $AC(\cdot)$  as  $\hat{F}$  and Eq. 12 as  $ExplanationLoss$  to measure the discrepancy between each subtree’s actual contribution  $AC_{st_k}$  and the model’s estimated contribution  $EC_{st_k}$ . Minimizing this loss ensures that the explanation accurately reflects how each subgraph influences the final cost. As a result, this technique helps the learning-based cost model maintain the transparency characteristic of classical summation-based approaches,

**Algorithm 1** Calculate contribution for each query plan node operation based on subtrees

**Input:** Query plan tree  $T$  with root node  $r$ , estimated contribution ratios  $EC_{st}(n)$  of the subtree rooted at each node  $n$   
**Output:** Estimated contribution ratios  $EC_{op}(n)$  for each node’s operation

- 1: **function** COMPUTE $EC(n)$
- 2:   **if**  $n$  is a leaf node **then**
- 3:      $EC_{op}(n) \leftarrow EC_{st}(n)$
- 4:   **else**
- 5:     **for** each child  $c$  of  $n$  **do**
- 6:       COMPUTE $EC(c)$
- 7:     **end for**
- 8:      $EC_{op}(n) \leftarrow EC_{st}(n) - \sum_{c \in Children(n)} EC_{st}(c)$
- 9:   **end if**
- 10: **end function**
- 11: COMPUTE $EC(r)$  //Start explanation from the root node

enabling users to understand its decisions and make precise, targeted adjustments.

### 3.3 A Robust Learning-to-Rank Cost Model Based on Uncertainty Quantification

In Section 2.3, we discussed the challenges of robust plan selection under inherent uncertainties and limitations in existing uncertainty quantification methods. To address these issues, we propose a robust learning-to-rank cost model that quantifies and integrates uncertainty into cost estimation. Rather than relying on purely numeric estimates or fixed strategies, our model employs a ranking loss with pairwise plan comparisons to learn how to adaptively combine cost and uncertainty into a single metric for plan selection. Learning from these comparisons, it identifies cheaper plans more reliably while factoring in uncertainty, thereby enhancing robustness in plan selection. Below, we detail how the model quantifies uncertainty and leverages pairwise comparisons during training.

**3.3.1 Uncertainty Quantification.** Real-world query plans often exhibit variability due to data uncertainty [12], which in ML can stem from noise in inputs or labels, or from low-dimensional features that fail to adequately learn the sample. During cost estimation, uncertainty can arise from various complex factors, including fluctuations in execution time due to changes in the load or hardware conditions of DBMSs when sample query plans are executing and the variability in the plan representations. In this work, we focus on this uncertainty and develop a method to quantify and utilize it.

A neural network can be designed to predict the parameters of the normal distribution [7], allowing it to predict not only the expected conditional value, but also the conditional variance of the target based on training data and the input sample. This functionality is achieved by integrating a secondary output branch into the original learning-based cost estimator that is tasked with variance prediction as shown in Figure 7. The optimization of this model involves maximizing the log-likelihood with a Gaussian prior [28], as demonstrated in the following uncertainty loss function:

$$UncertaintyLoss = \frac{1}{N} \sum_{i=1}^N \left( \frac{\log \sigma_{p_i}^2}{2} + \frac{(y_{p_i} - \mu_{p_i})^2}{\sigma_{p_i}^2} \right) \quad (13)$$

where for the  $i$ -th plan embedding as input,  $\mu_{p_i}$  is predicted by the first branch of the estimator and represents the expected value of the estimated cost,  $\sigma_{p_i}^2$  is from the second branch and reflects the expected variance as the data uncertainty, and  $y_{p_i}$  stands for the label (actual cost) of the input plan. Minimizing this loss function, we can obtain both the estimated cost and the expected conditional variance for a given plan embedding, enabling effective uncertainty quantification for the subsequent plan selection phase.

**3.3.2 Learning-to-Rank Pairwise Plan Comparison.** As discussed in Section 2, most existing uncertainty-aware cost estimation models usually apply the obtained uncertainty and estimated costs to the fixed plan selection strategy independently of the model training phase, preventing self-improvement based on selection outcomes. To address this, we propose a novel learning-based cost model architecture as shown in Figure 7 that uses a ranking loss function with plan pairs as inputs, allowing the model to adaptively integrate uncertainty and cost estimates. This approach improves the ability

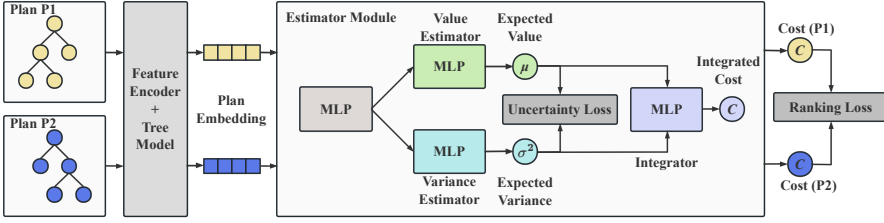


Figure 7: The architecture of the learning-to-rank robust cost model

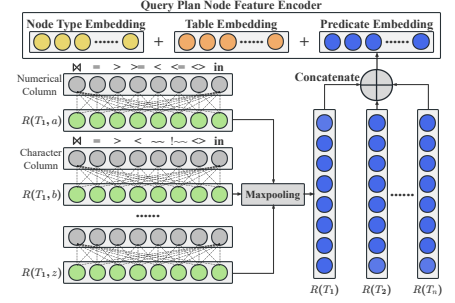


Figure 8: Query plan node feature encoder

to distinguish the actual performance of different plans, thereby providing more robust plan selection performance.

**Learning-based Integration.** We integrate the estimated mean  $\mu_p$  and variance  $\sigma_p^2$  from the estimator module to compute each plan  $p$ 's integrated cost  $C_p$ . Specifically,

$$C_p = \alpha \left( W \begin{bmatrix} \mu_p \\ \sigma_p^2 \end{bmatrix} + b \right) \quad (14)$$

where  $W$  is weight matrices,  $b$  is bias vectors, and  $\alpha$  is an activation function (e.g., Sigmoid). This approach allows the model to adapt the integration process to specific workload characteristics.

**Pairwise Plan Comparison.** In addition to learning based on prediction cost accuracy, our cost estimator module also learns from pairwise plan comparisons with binary labels indicating which one is better for each pair. Given a query plan set  $P$  of size  $N$ , a pair of plans  $(p_i, p_j)$  where  $\{p_i, p_j\} \in P$ , with estimated integrated cost  $(C_{p_i}, C_{p_j})$  and actual execution cost  $(y_{p_i}, y_{p_j})$ , a specified designed margin ranking loss function enables the model to learn from the comparative results, as follows:

$$RankingLoss = \sum_{i=1}^N \sum_{j=i+1}^N \exp(\max(0, -y_{p_{ij}} \cdot (C_{p_i} - C_{p_j}) + \text{margin}))$$

$$\text{where } y_{p_{ij}} = \begin{cases} 1, & y_{p_i} > y_{p_j} \\ -1, & y_{p_i} \leq y_{p_j} \end{cases} \quad (15)$$

Here, the "margin" is a hyperparameter that sets a threshold distance between plan costs to enhance differentiation and adjust misclassification penalties during learning. Therefore, the complete loss function of this cost model is defined as:

$$Loss = UncertaintyLoss(Eq. 13) + RankingLoss(Eq. 15) \quad (16)$$

Our learning-to-rank cost model addresses the robust plan selection problem in Section 2.3 by first providing two specialized output branches: one branch served as  $f$  to estimate cost and another as  $u$  to quantify uncertainty. We then introduce a learning-based integration function (Eq. 14) as  $h$  that adaptively balances these two outputs. By incorporating pairwise plan comparisons into training, for a plan  $p$ , the model automatically combines  $f(p)$  and  $u(p)$  into a single value to rank candidate plans, precisely capturing the core requirement of plan selection: comparing and choosing the most robust plan under inherent uncertainty. Consequently, our cost model not only strengthens overall robustness through uncertainty-aware training but also supports flexible utilization of quantified

uncertainty in plan selection, thereby offering a comprehensive solution to the challenges outlined in the problem statement.

## 4 MODEL ARCHITECTURE

By integrating the three techniques in Section 3, we propose Reqo, a learning-based cost model that improves cost estimation accuracy, explainability, and plan selection robustness. Figure 9 shows its architecture, consisting of a plan feature encoder and three modules (representation learning, estimation, and explanation). Sections 4.1 to 4.5 detail each component and the training process.

### 4.1 Plan Feature Encoding

A query execution plan contains details about the operators used to access and join data, their physical implementations, sequences, and the tables and columns involved. To transform this complex information into fixed-length node features for the tree model, we propose a plan encoder inspired by RTOS [39]. As shown in Figure 8, each node feature comprises three parts:

**Node Type Embedding.** We perform one-hot encoding of the node types (e.g., Hash Join, Index Scan) and pass them through a fully connected layer to obtain the node type embedding  $E(\text{nodetype})$ .

**Table Embedding.** One-hot encoding is applied to all tables used in the node's operation to obtain  $E(\text{table})$ , ensuring no loss of information even if there are no related predicates.

**Predicate Embedding.** For numerical columns, predicate operations are classified into eight cases (e.g.,  $\neq, =, >, <, \geq, \leq, \text{in}$ ). Each column  $c$  is represented by a feature vector  $F(c)$  of length eight, capturing these cases. The predicate values are normalized based on the column's value range in the database. For non-numerical columns like strings, we use word2vec [25] to convert characters into numerical values. Each column has a dedicated matrix  $M(c)$  to process  $F(c)$  and generate the column embedding  $E(c) = F(c) \times M(c)$ .

Max pooling is performed on all column embeddings of the same table to obtain the table embedding  $E(t)$ . To avoid information loss, we concatenate the embeddings of all tables to form the predicate embedding  $E(\text{predicate})$ . Finally, we concatenate  $E(\text{nodetype})$ ,  $E(\text{table})$ , and  $E(\text{predicate})$  to get the node feature.

### 4.2 Representation Learning Module

The representation learning module generates plan-level embeddings from the encoded query plan tree. We employ our proposed tree model BIGG, which consists of four bidirectional GNN layers and a GRU aggregation layer (detailed in Section 3.1). This module

takes a vectorized query plan tree as input. Each bidirectional GNN layer transforms it into two single-directional tree graphs (with opposite edge directions) that are processed by independent TransformerConv [33] layers. Their node features are then weighted recombined into a single output tree. After 4 such layers, the tree is converted into a node sequence via post-order traversal and processed by a GRU aggregation operator [1], which aggregates node information into the final plan representation.

### 4.3 Estimation Module

The estimation module (detailed in Section 3.3) processes the embedding from the representation learning module. This representation is input into a multi-layer perceptron (MLP) with 3 FC layers. The output then feeds into two separate branches, each consisting of an MLP with 3 layers. The first branch uses a Sigmoid activation function to produce a normalized expected execution time, while the second employs a SoftPlus function to generate a non-negative variance representing uncertainty. These outputs are integrated by an MLP with 2 layers and a Sigmoid activation, yielding an integrated value, which is used for plan comparison or selection.

### 4.4 Explanation Module

The explanation module extracts subtrees from the vectorized query plan tree using the mechanism detailed in Section 3.2.1. These subtrees are processed by the representation module to obtain subplan-level embeddings. Each subtree embedding is then concatenated with the complete plan embedding and inputs into the explainer, which consists of an MLP with 4 FC layers and a Sigmoid activation function. The explainer predicts the contribution ratio (ranging from 0 to 1) of each subtree toward the predicted execution time of the entire plan. These contribution values are used to explain the impact of specific subgraphs and nodes on the final prediction.

### 4.5 Model Training and Testing

The training of Reqq requires input in the form of query plan pairs, using the actual execution times of these plans and their subplans as labels. The model compares integrated values (execution time estimates and uncertainty) between different plans, leveraging ranking loss (Eq. 15) to learn from these comparison results. The estimation module is trained with both uncertainty loss (Eq. 13) and ranking loss, while the explanation module uses the explanation loss (Eq. 12). The explanation module is optional: If the model does not require explainability, training only uses the loss function (Eq. 16). When the explainability module is required, the overall loss function becomes the sum of the three losses, as shown in Eq. 17.

$$\begin{aligned} Loss = & \text{UncertaintyLoss}(Eq. 13) + \text{RankingLoss}(Eq. 15) \\ & + \text{ExplanationLoss}(Eq. 12) \end{aligned} \quad (17)$$

Reqq does not require inputs to be paired during the testing phase. After training, plans can be directly ranked based on the integrated value produced by the estimation module, thereby achieving the prediction plan selection incorporating uncertainty.

## 5 EXPERIMENTAL STUDY

We experimentally evaluate and compare Reqq’s performance with state-of-the-art cost models. The experimental setup is described

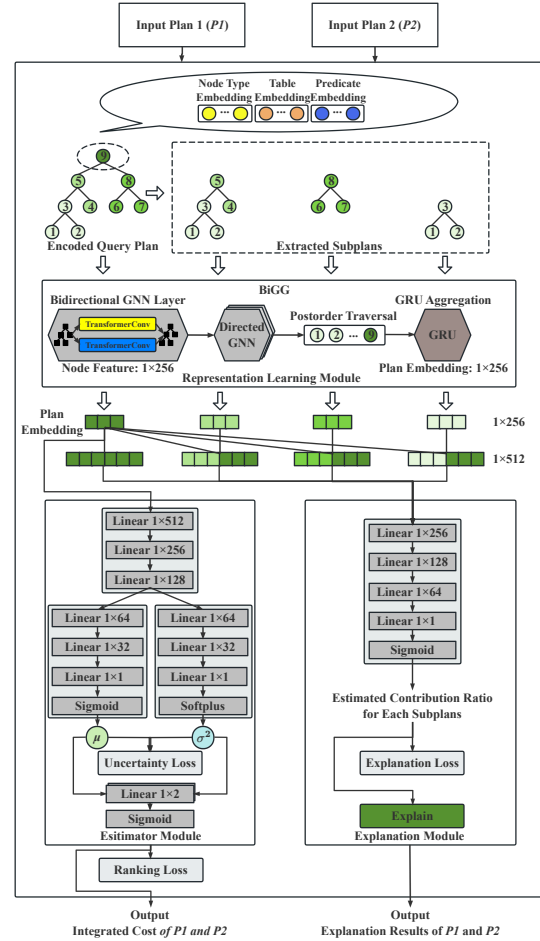


Figure 9: The complete architecture of Reqq

in Section 5.1, followed by methodology and metrics in Section 5.2. Section 5.3 analyzes the results on cost estimation, plan selection, robustness, and explainability. Experimental findings show Reqq consistently outperforms existing approaches, demonstrating its effectiveness in real-world database environments.

### 5.1 Experimental Setup

All experiments were conducted on a Linux server (8-core Intel Silver 4216 CPU @ 2.1GHz, 128GB RAM, 32GB NVIDIA V100 GPU). PostgreSQL 15.1 was used to compile and execute queries for workload generation. The prototype was implemented in Python 3.10 using PyTorch [29], with hyperparameters tuned via Ray Tune [17]. ADAM [13] was used as the optimizer during training, with dropout and early stopping applied to prevent overfitting. All experimental results were averaged over 10-fold cross-validation.

**Benchmarks.** We evaluate all the query optimizer cost models on four widely used benchmarks:

The **STATS dataset and STATS-CEB workload** [8] include 8 tables from the Stats Stack Exchange network with more complex data distributions than IMDB. STATS-CEB provides 146 query templates with varying join sizes and types. We generate a workload of 3,000 queries by adding random predicates to these templates.



The *IMDB dataset and JOB-light workload* [16] contains 21 tables and 70 real-world query templates ranging from 2 to 5 joins. Using the same method described above, we generate 2,600 queries.

The *TPC-H benchmark* [30] is designed to test database performance with complex business queries. We used TPC-H 3.0.1 to generate a 10 GB database with 8 tables and 61 columns. From its 22 query templates, we produce 1,100 queries by varying predicates.

The *TPC-DS benchmark* [31] is an industrial-standard benchmark for evaluating database performance. We use TPC-DS 3.2 to generate a 10 GB database with 25 tables and 429 columns, supporting more complex query patterns than the other benchmarks. Due to the limited complexity of built-in templates, we use a random query generator to produce 8,000 queries. The queries are generated by parameters such as join number, join types (e.g., inner, outer, anti-joins) and the number of predicates. Each query includes up to 10 joins, 3 join predicates per join, and 5 local predicates per table.

**Dataset Generating and Preprocessing.** We build our experimental datasets from these workloads. Each query is compiled in PostgreSQL using 13 different hints inspired by Bao [23] that constrain join and access operators. Each sample in the dataset comprises candidate query plans generated for the same query using these hints. We take PostgreSQL’s compiled query plans’ execution times as labels for cost estimation and plan selection. We also collect execution times of each plan’s extracted subtrees for explanation labels (Section 3.2.1). To conserve resources and speed up training, we exclude individual leaves as subtrees. To reduce skewness of the execution time values and ensure alignment with the output of model’s Sigmoid activation, we apply a natural log transformation followed by min-max scaling, mapping each execution time  $y$  into  $[0, 1]$  using the training data’s minimum and maximum.

## 5.2 Experimental Methodology

**Comparison.** We compare our proposed model, Reqa, against the classical RDBMS optimizer PostgreSQL and three recent works: Bao [23], Lero [45], and Roq [12]. Bao is selected for its advanced performance, Lero for its learning-to-rank mechanism, and Roq for its approach to quantifying uncertainty for robust plan selection. These comparisons allow us to evaluate improvements across different aspects based on state-of-the-art mechanisms.

*PostgreSQL* serves as the baseline, representing the performance of commercial query optimizers. We use the plans selected by PostgreSQL’s estimated cost for plan selection and explainability.

*Bao* is a learned query optimizer that enhances traditional optimizers by applying hints and reinforcement learning. We focus on its cost model, which predicts execution time by processing the vectorized plan tree through TCNN and MLP.

*Lero* is a learning-to-rank query optimizer. Similar to Bao in plan encoding, Lero trains its cost model to classify which of two plans is better rather than predicting numerical values. Thus, it is excluded from our cost estimation accuracy comparison.

*Roq* is a robust risk-aware query optimization framework with a GNN-based query-level encoder and a plan encoding similar to Bao. Its cost model estimates execution time and uncertainty, and applies them in fixed robust plan selection strategies.

*Reqa* is our proposed model and is divided into segments for an ablation study. The base model (BiGG + single-branch MLP with

MSE loss, no explanation) serves as a benchmark. We then add uncertainty quantification (base+unc.) to observe the impact of using *UncertaintyLoss* and dual-branch MLP without applying it to plan selection. Next, we integrate estimated execution time and uncertainty using a fixed value (base+unc.+ $f_{fixed}$ ) for plan selection to evaluate whether the ranking-based approach (base+unc.+ $f_{earned}$  or Reqa w/o expl.) enhances the robustness. We also introduce the explanation module (Reqa w/ expl.) to assess its impact. Throughout, "Reqa" refers to the model that contains all modules.

**Evaluation Metrics.** We employ six evaluation metrics:

**1. Prediction Error:** We evaluate cost estimation performance using Q-Error [26], defined as  $Q-Error = \max(y_{et}, y_{at}) / \min(y_{et}, y_{at})$ , where  $y_{et}$  and  $y_{at}$  are the estimated and actual execution times.

**2. Correlation:** We use Spearman’s rank correlation to measure the relationship between estimated and actual execution time, with values closer to 1 indicating a stronger correlation. Unlike Pearson’s coefficient, it is less sensitive to outliers and scale differences, making it suitable for measurements that vary greatly in magnitude.

**3. Total Runtime Ratio:** This ratio is computed by dividing the sum of actual execution times for optimizer-selected plans by the sum of actual execution times for optimal plans across all queries, offering an evaluation of overall plan selection performance.

**4. Plan Suboptimality:** For a set of candidate execution plans  $p$  for the same query, we rank them by actual execution time  $ET(\cdot)$  and identify the optimal plan  $p_o$  with the shortest execution time. The suboptimality of a plan  $p_i \in p$  is defined as:

$$\text{Plan Suboptimality} = \frac{ET(p_i)}{ET(p_o)} \quad (18)$$

This metric ranges from  $[1, \infty)$  and reflects the model’s ability to select optimal plans. Analyzing the distribution, especially the worst cases, helps assess the model’s robustness in plan selection [6].

**5. Explanation Top-K Subgraph Accuracy:** This metric assesses the model’s accuracy in identifying the most influential subgraphs contributing to the final prediction. Each query plan is divided into minimal, non-overlapping subgraphs, each containing at most one parent node and its children if they are leaf nodes. If a parent has a non-leaf child, that child is excluded from the parent’s subgraph and becomes the parent in a separate subgraph. Ranking these subgraphs by their contribution, the metric checks whether the top-K model selected most influential subgraphs  $S_{pred,k}$  match the actual top-K subgraphs  $S_{actual,k}$ . Let  $\mathbb{I}$  be an indicator function returning 1 if the subgraphs match and 0 otherwise. Specifically,

$$\text{Expl. Top-K Subgraph Acc} = \mathbb{I}\left(\{S_{pred,k}^i = S_{actual,k}^i\}_{k=1}^K\right) \quad (19)$$

**6. Explanation Top-K Subgraph Influence Ratio:** This metric evaluates the model’s ability to identify most influential subgraphs by comparing the sum of actual contributions from the top-K model-selected subgraphs  $S_{pred,k}$  against the top-K actual subgraphs  $S_{actual,k}$ . Formally,

$$\text{Expl. Top-K Subgraph Infl. Ratio} = \frac{\sum_{k=1}^K AC(S_{pred,k})}{\sum_{k=1}^K AC(S_{actual,k})} \quad (20)$$

Subgraphs are partitioned the same as above. Unlike binary accuracy, this ratio captures cases where the model’s chosen subgraphs contribute significantly, even if they are not the top-K subgraphs, providing a more comprehensive evaluation of explainability.

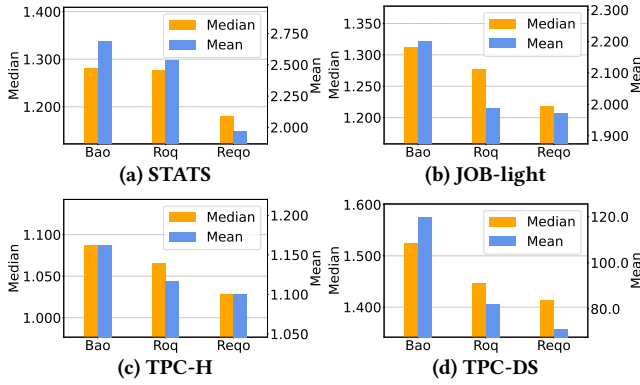


Figure 10: Comparing the cost estimation performance (Median and mean Q-error) of models across different workloads

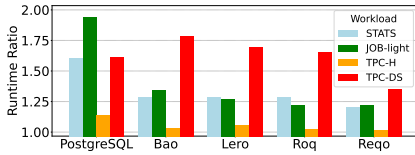


Figure 11: Comparing the total runtime ratio performance (ratio of the total runtime of model selected plans to actual optimal plans) of various models across different workloads

## 5.3 Experimental Results

**5.3.1 Comparison for Cost Estimation.** Figure 10 demonstrate that Reqq consistently outperforms Bao and Roq across all datasets in terms of Q-error and Spearman’s correlation metrics. Reqq achieves lower Q-Error values at various percentiles and higher Spearman’s correlation coefficients, indicating superior cost estimation performance. Notably, in complex workloads like TPC-DS, Reqq still excels, showcasing its effectiveness in handling challenging scenarios with more complex and deeper query plans. These results confirm Reqq’s advancement over existing models and its effectiveness in both simple and complex query optimization tasks.

**5.3.2 Comparison for Plan Selection.** The runtime results (Figure 11) show the models’ plan selection performance across the entire workload. Reqq consistently surpasses other models, demonstrating substantial performance enhancements. Notably, in the more complex TPC-DS workload, models like Bao, Lero, and Roq do not perform as well as PostgreSQL in terms of total runtime, despite exhibiting better performance in simpler workloads. In contrast, Reqq’s advanced feature encoder, the powerful representation capabilities of BiGG, and the ranking-based uncertainty quantification mechanism ensure superior performance even with complex query plans. Specifically, in optimizing total runtime ratio, Reqq achieves performance enhancements of 16.6% over PostgreSQL, 24.6% over Bao, 20.4% over Lero, and 18.6% over Roq. These results underscore Reqq’s efficiency in handling complex query scenarios, highlighting its superiority in runtime performance optimization.

**5.3.3 Ablation Study.** To analyze the impact of our proposed techniques on cost estimation and plan selection, we conducted an ablation study on the TPC-DS workload. Figure 12a shows variations in Spearman’s correlation for different Reqq configurations versus other cost models. All learning-based models significantly

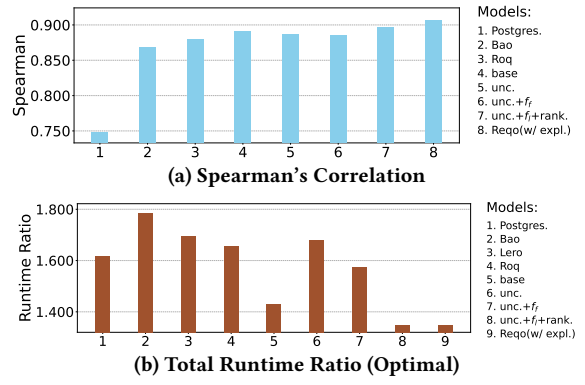


Figure 12: Comparison of Spearman’s Correlation and Total Runtime Ratio (Optimal) on TPC-DS

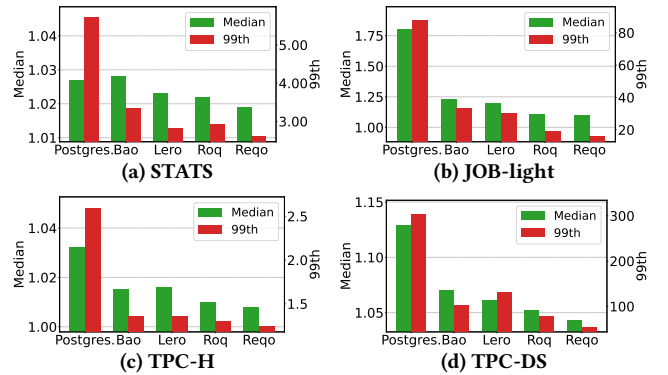


Figure 13: Plan suboptimality performance of various models across different workloads

outperform PostgreSQL’s traditional cost model. Our base model (base), which leverages BiGG as tree model, surpasses both Bao and Roq without additional mechanisms, showcasing BiGG’s powerful representation learning and more accurate execution time estimation capability. Adding uncertainty quantification (base+unc. and base+unc.+ $f_{fixed}$ ) enhances plan selection robustness by quantifying uncertainty during cost estimation, though it slightly reduces estimation accuracy. Incorporating the learning-to-rank mechanism (base+unc.+ $f_{learned}$ ) addresses this trade-off and further improves cost estimation performance, ensuring that our robust cost model maintains strong accuracy while enhancing robustness.

For plan selection performance, Figure 12b presents total runtime ratio results under the same TPC-DS workload. Although the base model already outperforms PostgreSQL and other learning-based models, enabling uncertainty quantification without applying it to plan selection (base+unc.) leads to reduced performance, also reflecting the trade-off between uncertainty and accuracy. Integrating uncertainty with a fixed parameter (base+unc.+ $f_{fixed}$ ) does improve performance, but still not to the level achieved by the base model. However, our learning-to-rank uncertainty-aware approach (base+unc.+ $f_{learned}$ ) further enhances runtime performance, surpassing the base model and confirming its effectiveness in improving plan selection performance.

**5.3.4 Comparison for Robustness.** We evaluate plan selection robustness via plan suboptimality, with results shown in Figure 13.

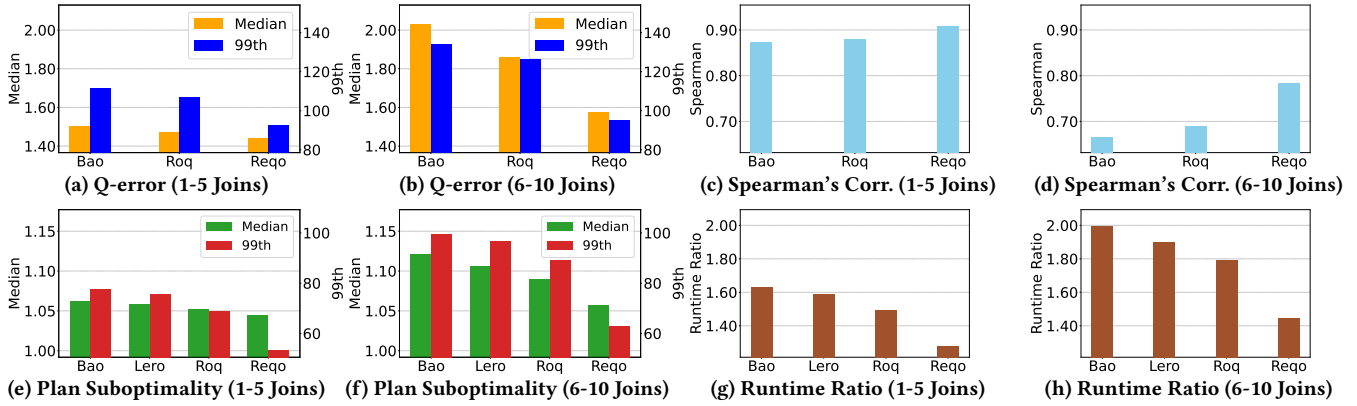


Figure 14: Performance metrics across TPC-DS in a workload shift task. The models are trained on TPC-DS workloads containing 4,500 queries with 1–5 joins and tested on two workloads: 500 queries with 1–5 joins and 500 queries with 6–10 joins

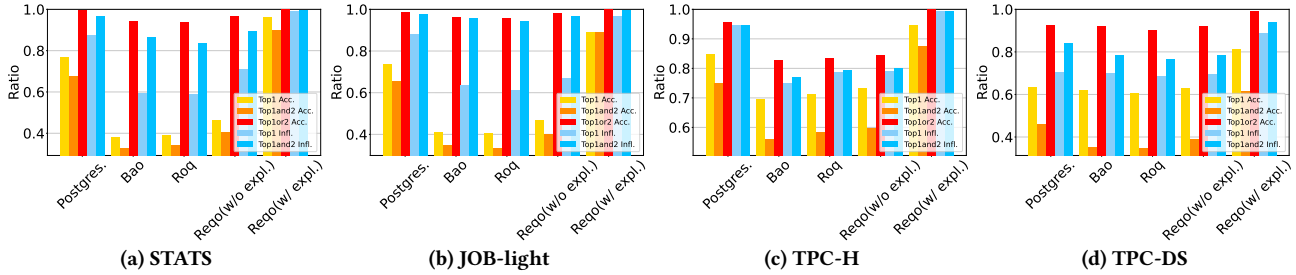


Figure 15: Comparing the explanation performance of models across different workloads. Top1 Acc, Top1and2 Acc, and Top1or2 Acc measure accuracy in identifying the most influential subgraph(s): Top1 Acc focuses on the single most significant subgraph, Top1and2 Acc on the top two subgraphs together, and Top1or2 Acc on correctly identifying either of the top two. Top1 Infl. and Top1and2 Infl. assess the influence ratio of the selected subgraphs relative to the actual most influential subgraph(s)

In simpler workloads, the performance gap among models is small, as baseline models generally make correct decisions. Nonetheless, Rejo still achieves the most accurate plan selection, particularly excelling at the 99th percentile tail and thus demonstrating superior robustness under worst-case scenarios. In the more complex TPC-DS workload, both Rejo and Roq leverage uncertainty quantification to enhance robustness and outperform other models. Rejo ultimately surpasses Roq through its ranking-based adaptive integration, confirming its stronger robustness in plan selection.

To further assess robustness, we conduct a workload shift experiment. Models are trained on queries with 1–5 joins and then separately tested on queries with 1–5 joins and 6–10 joins, thereby examining their adaptability to more complex and previously unseen workloads. Figure 14 shows that Rejo achieves the best results across all metrics in the simpler workload and, despite a performance decline in the more complex scenario (as observed for all models), Rejo experiences the smallest drop. Moreover, its relative advantage over Bao and Roq becomes more pronounced as complexity increases. Combined with its superior tail-end performance in Q-error and plan suboptimality, these findings confirm that Rejo demonstrates exceptional robustness and outperforms other state-of-the-art models under challenging conditions.

**5.3.5 Comparison for Explainability.** From Figure 15, we observe that the traditional PostgreSQL optimizer, despite underperforming in previous experiments compared to learning-based models, demonstrates relatively good explainability. Learning-based cost models, including our proposed Rejo (without the explainability technique), excel in cost estimation accuracy and robustness but fall short of PostgreSQL in explainability. The main reason is that these models prioritize to predict cost estimates, rather than identifying specific subgraphs that significantly influence the embedding and drive the model’s predictions. This issue is a common limitation across nearly all current learning-based cost models: they provide accurate cost estimates but lack the ability to explain why certain decisions are made, hindering targeted query optimization.

In contrast, the classical optimizer used by PostgreSQL bases its cost predictions on detailed cost statistics for each node operation in the plan, enabling it to clearly show its decision-making process and therefore performs better in this experiment. The experimental results demonstrate that, without our proposed explainability technique, the learning-based cost models perform worse than PostgreSQL in almost all explanation evaluation metrics. In particular, there is a clear gap in accuracy when the learning-based cost model is required to simultaneously identify the two most influential subgraphs in order. This suggests that although these cost models can provide vague explanations, they struggle to precisely pinpoint

the contributions of subgraphs. This lack of precise explanations presents challenges for trusting the results of query optimization in practice, highlighting the necessity of integrating an explainability mechanism into the query plan cost prediction process.

However, due to limitations in the traditional optimizer, PostgreSQL’s cost estimates for each node are not accurate, leading to insufficient explanation performance. Integrating explainability techniques enhances the transparency and accuracy of cost predictions made by learning-based cost models, aligning them more closely with traditional models like PostgreSQL. Experimental findings demonstrate that Reqo, when equipped with the explainability technique, surpasses other models across all evaluative metrics. Specifically, in simpler scenarios, it achieves perfect scores in the Top1or2 accuracy ratio and nearly perfect scores in the Top1and2 influence ratio, effectively identifying and quantifying the most influential subgraphs. Even in the challenging TPC-DS workload, Reqo shows substantial improvements, with explanation accuracy metrics increasing by nearly 20% and explanation influence ratios exceeding a 10% increase compared to PostgreSQL.

Therefore, our subtree-based explainability technique demonstrably improves the cost model’s transparency. The cost model integrated with our explainability technique can adaptively learn the correlation between the embeddings of subgraphs and the complete query plan during training. This enables more precise estimation of the subgraphs’ contributions to execution time predictions, providing a more accurate explanation of the results. Additionally, the inclusion of explanation loss allows Reqo to focus more on generating embeddings, meaning that the greater a subgraph’s contribution, the stronger the similarity between its embedding and the complete plan’s embedding. This mechanism not only improves the explainability of the embeddings but also enhances the model’s ability to effectively process query plans of varying sizes.

As shown in Figure 12, integrating explainability module does not compromise Reqo’s cost estimation or robustness performance; instead, it slightly enhances them. This effect arises partly from the explainability technique’s ability to preserve the entire original model architecture while enhancing the model’s understanding and representation of query plans. Additionally, the subtree extraction process for explainability optimizes the utilization of information within the query plan, further contributing to this enhancement.

## 6 RELATED WORK

This study primarily involves three aspects of query optimization cost models, focusing on learning-based technologies for tree models and robustness techniques for query optimizers.

**Learning-based Tree Model.** RNN-based models like LSTM [9] are common in learning-based query optimization [35, 40] due to their ability to capture long-term dependencies but require transforming trees into sequences, resulting in loss of structural information. Models such as Saturn [21] and QueryFormer [43] use self-attention mechanisms to enhance plan representation but still convert query plans into sequences. Tree-specific models like Tree-LSTM [36] and Tree-CNN [27] process tree-structured data directly, preserving structural relationships and improving feature aggregation. However, they still do not work well with deep query plans [2]. BiGG addresses these issues by combining bidirectional GNN with

GRU, demonstrating superior query plan representation and significant performance improvements in cost estimation and plan selection tasks compared to other tree models [2].

**Learning-based Robustness Techniques.** Most learning-based query optimizer cost models focus on achieving accurate cost estimates using supervised or reinforcement learning with query plan cardinality or execution time as labels. Although generally effective, they do not explicitly target robustness or incorporate mechanisms to quantify and leverage the inherent uncertainty. Although some studies like [23, 24] indicate a degree of robustness to estimation errors or limit the worst-case scenario, inherent predictive uncertainties persist without systematic methods for quantification. Recent research proposes solutions for quantifying uncertainty. Studies such as [12, 19, 38, 41, 42] employ Gaussian negative log-likelihood [28] and [5] introduce spectral normalized neural Gaussian processes (SNGP) [20] in cost model training to estimate data uncertainty by predicting variances along with cost predictions. Others [4, 12, 19, 41] employ Bayesian Neural Networks or approximate probabilistic neural networks such as Monte Carlo Dropout to assess model uncertainty. However, these approaches integrate learning-based cost models with traditional optimizers, using uncertainty quantification to discard plans with high uncertainty or determine if they fall back to conventional methods. While these methods consider uncertainty when selecting optimal plans to achieve more robust performance, plan selection remains independent of the model’s training phase. Current strategies rely on predefined rules, such as uncertainty thresholds, making the models less adaptable and hindering their ability to learn from plan selection results to improve the rules.

Our proposed model, Reqo, addresses these limitations by automatically learning to integrate cost estimates and uncertainty without requiring human fine-tuning or preset rules. In addition, Reqo offers an advantage over other learning-to-rank cost models, such as Lero [45] or Leon [4], which do not support numerical cost estimation and instead categorize paired query plans to determine the better plan. Such models require pairing various candidate plans and performing multiple comparison rounds to identify the optimal plan during selection. In contrast, our method benefits from the learning-to-rank mechanism during training with paired plans but eliminates the need for multi-round pairwise comparisons during testing and reduces inference overhead in complex situations.

## 7 CONCLUSION

We introduce Reqo, a novel cost model that integrates a BiGG tree model (bidirectional GNN and GRU) for enhanced representation, a learning-to-rank uncertainty-aware cost model for robust plan selection, and a subtree-based explainability technique. While achieving top-tier cost estimation accuracy, Reqo adaptively integrates cost estimates with uncertainties through pairwise plan comparisons, thereby improving robustness. Our explainability technique enhances the transparency of learning-based cost models through a tailored subgraph extraction method and a learning-based explainer, making Reqo the first learning-based cost model capable of explaining its cost estimates. Through extensive experiments, Reqo demonstrates superior accuracy, robustness, and explainability, outperforming state-of-the-art cost models in all three aspects.

## REFERENCES

- [1] David Buterez, Jon Paul Janet, Steven J Kiddle, Dino Oglic, and Pietro Liò. 2022. Graph neural networks with adaptive readouts. *Advances in Neural Information Processing Systems* 35 (2022), 19746–19758.
- [2] Baoming Chang, Amin Kamali, and Verena Kantere. 2024. A Novel Technique for Query Plan Representation Based on Graph Neural Nets. In *Big Data Analytics and Knowledge Discovery: 26th International Conference, DaWaK 2024, Naples, Italy, August 26–28, 2024, Proceedings* (Naples, Italy). Springer-Verlag, Berlin, Heidelberg, 299–314. [https://doi.org/10.1007/978-3-031-68323-7\\_25](https://doi.org/10.1007/978-3-031-68323-7_25)
- [3] Tianyi Chen, Jun Gao, Hedui Chen, and Yaofeng Tu. 2023. LOGER: A Learned Optimizer Towards Generating Efficient and Robust Query Execution Plans. *Proceedings of the VLDB Endowment* 16, 7 (March 2023), 1777–1789. <https://doi.org/10.14778/3587136.3587150>
- [4] Xu Chen, Haitian Chen, Zibo Liang, Shuncheng Liu, Jinghong Wang, Kai Zeng, Han Su, and Kai Zheng. 2023. LEON: A New Framework for ML-Aided Query Optimization. *Proceedings of the VLDB Endowment* 16, 9 (May 2023), 2261–2273. <https://doi.org/10.14778/3598581.3598597>
- [5] Lyric Doshi, Vincent Zhuang, Gaurav Jain, Ryan Marcus, Haoyu Huang, Deniz Altinbiken, Eugene Brevdo, and Campbell Fraser. 2023. Kepler: Robust Learning for Parametric Query Optimization. *Proceedings of the ACM on Management of Data* 1, 1, Article 109 (May 2023), 25 pages. <https://doi.org/10.1145/3588963>
- [6] Anshuman Dutt and Jayant R. Haritsa. 2014. Plan bouquets: query processing without selectivity estimation. In *Proceedings of the 2014 ACM SIGMOD International Conference on Management of Data* (Snowbird, Utah, USA) (SIGMOD '14). Association for Computing Machinery, New York, NY, USA, 1039–1050. <https://doi.org/10.1145/2588555.2588566>
- [7] Philippe Flajolet and G Nigel Martin. 1985. Probabilistic counting algorithms for data base applications. *Journal of computer and system sciences* 31, 2 (1985), 182–209.
- [8] Yuxing Han, Ziniu Wu, Peizhi Wu, Rong Zhu, Jingyi Yang, Liang Wei Tan, Kai Zeng, Gao Cong, Yanzhao Qin, Andreas Pfadler, Zhengping Qian, Jingren Zhou, Jiangneng Li, and Bin Cui. 2021. Cardinality estimation in DBMS: a comprehensive benchmark evaluation. *Proceedings of the VLDB Endowment* 15, 4 (Dec. 2021), 752–765. <https://doi.org/10.14778/3503585.3503586>
- [9] Sepp Hochreiter and Jürgen Schmidhuber. 1997. Long Short-Term Memory. *Neural Computation* 9, 8 (Nov. 1997), 1735–1780. <https://doi.org/10.1162/neco.1997.9.8.1735>
- [10] Yannis Ioannidis. 2003. The history of histograms (abridged). In *Proceedings of the 29th International Conference on Very Large Data Bases - Volume 29* (Berlin, Germany) (VLDB '03). VLDB Endowment, 19–30.
- [11] Laurent Valentin Jospin, Hamid Laga, Farid Boussaid, Wray Buntine, and Mohammed Bannamoun. 2022. Hands-On Bayesian Neural Networks—A Tutorial for Deep Learning Users. *IEEE Computational Intelligence Magazine* 17, 2 (2022), 29–48. <https://doi.org/10.1109/MCI.2022.3155327>
- [12] Amin Kamali, Verena Kantere, Calisto Zuzarte, and Vincent Corvinnelli. 2024. Roq: Robust Query Optimization Based on a Risk-aware Learned Cost Model. *arXiv preprint arXiv:2401.15210* (2024).
- [13] Diederik P Kingma and Jimmy Ba. 2014. Adam: A method for stochastic optimization. *arXiv preprint arXiv:1412.6980* (2014).
- [14] Thomas N Kipf and Max Welling. 2016. Semi-supervised classification with graph convolutional networks. *arXiv preprint arXiv:1609.02907* (2016).
- [15] Alexander Kraskov, Harald Stögbauer, and Peter Grassberger. 2004. Estimating mutual information. *Physical Review E—Statistical, Nonlinear, and Soft Matter Physics* 69, 6 (2004), 066138.
- [16] Viktor Leis, Andrey Gubichev, Atanas Mirchev, Peter Boncz, Alfons Kemper, and Thomas Neumann. 2015. How good are query optimizers, really? *Proceedings of the VLDB Endowment* 9, 3 (Nov. 2015), 204–215. <https://doi.org/10.14778/2850583.2850594>
- [17] Richard Liaw, Eric Liang, Robert Nishihara, Philipp Moritz, Joseph E Gonzalez, and Ion Stoica. 2018. Tune: A Research Platform for Distributed Model Selection and Training. *arXiv preprint arXiv:1807.05118* (2018).
- [18] Zachary C. Lipton. 2018. The Mythos of Model Interpretability: In machine learning, the concept of interpretability is both important and slippery. *Queue* 16, 3 (June 2018), 31–57. <https://doi.org/10.1145/3236386.3241340>
- [19] Jie Liu, Wenqian Dong, Qingqing Zhou, and Dong Li. 2021. Fauce: fast and accurate deep ensembles with uncertainty for cardinality estimation. *Proceedings of the VLDB Endowment* 14, 11 (July 2021), 1950–1963. <https://doi.org/10.14778/3476249.3476254>
- [20] Jeremiah Zhe Liu, Shreyas Padhy, Jie Ren, Zi Lin, Yeming Wen, Ghassen Jerfel, Zachary Nado, Jasper Snoek, Dustin Tran, and Balaji Lakshminarayanan. 2023. A simple approach to improve single-model deep uncertainty via distance-awareness. *Journal of Machine Learning Research* 24, 1, Article 42 (Jan. 2023), 63 pages.
- [21] Shuncheng Liu, Xu Chen, Yan Zhao, Jin Chen, Rui Zhou, and Kai Zheng. 2022. Efficient Learning with Pseudo Labels for Query Cost Estimation. In *Proceedings of the 31st ACM International Conference on Information & Knowledge Management* (Atlanta, GA, USA) (CIKM '22). Association for Computing Machinery, New York, NY, USA, 1309–1318. <https://doi.org/10.1145/3511808.3557305>
- [22] Jiaqi Ma, Weijing Tang, Ji Zhu, and Qiaozhu Mei. 2019. A flexible generative framework for graph-based semi-supervised learning. Curran Associates Inc., Red Hook, NY, USA.
- [23] Ryan Marcus, Parimarjan Negi, Hongzi Mao, Nesime Tatbul, Mohammad Alizadeh, and Tim Kraska. 2021. Bao: Making Learned Query Optimization Practical. In *Proceedings of the 2021 International Conference on Management of Data* (Virtual Event, China) (SIGMOD '21). Association for Computing Machinery, New York, NY, USA, 1275–1288. <https://doi.org/10.1145/3448016.3452838>
- [24] Ryan Marcus, Parimarjan Negi, Hongzi Mao, Chi Zhang, Mohammad Alizadeh, Tim Kraska, Olga Papaemmanouil, and Nesime Tatbul. 2019. Neo: a learned query optimizer. *Proceedings of the VLDB Endowment* 12, 11 (July 2019), 1705–1718. <https://doi.org/10.14778/3342263.3342644>
- [25] Tomas Mikolov, Kai Chen, Greg Corrado, and Jeffrey Dean. 2013. Efficient estimation of word representations in vector space. *arXiv preprint arXiv:1301.3781* (2013).
- [26] Guido Moerkotte, Thomas Neumann, and Gabriele Steidl. 2009. Preventing bad plans by bounding the impact of cardinality estimation errors. *Proceedings of the VLDB Endowment* 2, 1 (Aug. 2009), 982–993. <https://doi.org/10.14778/1687627.1687738>
- [27] Lili Mou, Ge Li, Lu Zhang, Tao Wang, and Zhi Jin. 2016. Convolutional neural networks over tree structures for programming language processing. In *Proceedings of the Thirtieth AAAI Conference on Artificial Intelligence* (Phoenix, Arizona) (AAAI'16). AAAI Press, 1287–1293.
- [28] D.A. Nix and A.S. Weigend. 1994. Estimating the mean and variance of the target probability distribution. In *Proceedings of 1994 IEEE International Conference on Neural Networks (ICNN'94)*, Vol. 1. 55–60 vol.1. <https://doi.org/10.1109/ICNN.1994.374138>
- [29] Adam Paszke, Sam Gross, Francisco Massa, Adam Lerer, James Bradbury, Gregory Chanan, Trevor Killeen, Zeming Lin, Natalia Gimelshein, Luca Antiga, et al. 2019. Pytorch: An imperative style, high-performance deep learning library. *Advances in neural information processing systems* 32 (2019).
- [30] Meikel Poess and Chris Floyd. 2000. New TPC benchmarks for decision support and web commerce. *SIGMOD Record* 29, 4 (Dec. 2000), 64–71. <https://doi.org/10.1145/369275.369291>
- [31] Meikel Poess, Raghunath Othayoth Nambiar, and David Walrath. 2007. Why you should run TPC-DS: a workload analysis. In *Proceedings of the 33rd International Conference on Very Large Data Bases* (Vienna, Austria) (VLDB '07). VLDB Endowment, 1138–1149.
- [32] Emanuele Rossi, Bertrand Charpentier, Francesco Di Giovanni, Fabrizio Frasca, Stephan Gunnemann, and Michael Bronstein. 2023. Edge Directionality Improves Learning on Heterophilic Graphs. *arXiv preprint arXiv:2305.10498* (2023).
- [33] Yunsheng Shi, Zhengjie Huang, Shikun Feng, Hui Zhong, Wenjin Wang, and Yu Sun. 2020. Masked label prediction: Unified message passing model for semi-supervised classification. *arXiv preprint arXiv:2009.03509* (2020).
- [34] Jost Tobias Springenberg, Aaron Klein, Stefan Falkner, and Frank Hutter. 2016. Bayesian optimization with robust Bayesian neural networks. In *Proceedings of the 30th International Conference on Neural Information Processing Systems* (Barcelona, Spain) (NIPS'16). Curran Associates Inc., Red Hook, NY, USA, 4141–4149.
- [35] Ji Sun and Guoliang Li. 2019. An end-to-end learning-based cost estimator. *Proceedings of the VLDB Endowment* 13, 3 (Nov. 2019), 307–319. <https://doi.org/10.14778/3368289.3368296>
- [36] Kai Sheng Tai, Richard Socher, and Christopher D. Manning. 2015. Improved Semantic Representations From Tree-Structured Long Short-Term Memory Networks. In *Proceedings of the 53rd Annual Meeting of the Association for Computational Linguistics and the 7th International Joint Conference on Natural Language Processing* (Volume 1: Long Papers), Chengqing Zong and Michael Strube (Eds.). Association for Computational Linguistics, Beijing, China, 1556–1566. <https://doi.org/10.3115/v1/P15-1150>
- [37] Ashish Vaswani, Noam Shazeer, Niki Parmar, Jakob Uszkoreit, Llion Jones, Aidan N. Gomez, Lukasz Kaiser, and Illia Polosukhin. 2017. Attention is all you need. In *Proceedings of the 31st International Conference on Neural Information Processing Systems* (Long Beach, California, USA) (NIPS'17). Curran Associates Inc., Red Hook, NY, USA, 6000–6010.
- [38] Xiang Yu, Chengliang Chai, Guoliang Li, and Jiabin Liu. 2022. Cost-Based or Learning-Based? A Hybrid Query Optimizer for Query Plan Selection. *Proceedings of the VLDB Endowment* 15, 13 (Sept. 2022), 3924–3936. <https://doi.org/10.14778/3565838.3565846>
- [39] Xiang Yu, Guoliang Li, Chengliang Chai, and Nan Tang. 2020. Reinforcement Learning with Tree-LSTM for Join Order Selection. In *2020 IEEE 36th International Conference on Data Engineering (ICDE)*. 1297–1308. <https://doi.org/10.1109/ICDE48307.2020.00116>
- [40] Haitao Yuan, Guoliang Li, Ling Feng, Ji Sun, and Yue Han. 2020. Automatic View Generation with Deep Learning and Reinforcement Learning. In *2020 IEEE 36th International Conference on Data Engineering (ICDE)*. 1501–1512.

<https://doi.org/10.1109/ICDE48307.2020.00133>

- [41] Kangfei Zhao, Jeffrey Xu Yu, Zongyan He, Rui Li, and Hao Zhang. 2022. Light-weight and Accurate Cardinality Estimation by Neural Network Gaussian Process. In Proceedings of the 2022 International Conference on Management of Data (Philadelphia, PA, USA) (SIGMOD '22). Association for Computing Machinery, New York, NY, USA, 973–987. <https://doi.org/10.1145/3514221.3526156>
- [42] Kangfei Zhao, Jeffrey Xu Yu, Zongyan He, Rui Li, and Hao Zhang. 2022. Light-weight and Accurate Cardinality Estimation by Neural Network Gaussian Process. In Proceedings of the 2022 International Conference on Management of Data (Philadelphia, PA, USA) (SIGMOD '22). Association for Computing Machinery, New York, NY, USA, 973–987. <https://doi.org/10.1145/3514221.3526156>
- [43] Yue Zhao, Gao Cong, Jiachen Shi, and Chunyan Miao. 2022. QueryFormer: a tree transformer model for query plan representation. Proceedings of the VLDB Endowment 15, 8 (April 2022), 1658–1670. <https://doi.org/10.14778/3529337.3529349>
- [44] Yue Zhao, Zhaodonghui Li, and Gao Cong. 2023. A Comparative Study and Component Analysis of Query Plan Representation Techniques in ML4DB Studies. Proceedings of the VLDB Endowment 17, 4 (Dec. 2023), 823–835. <https://doi.org/10.14778/3636218.3636235>
- [45] Rong Zhu, Wei Chen, Bolin Ding, Xingguang Chen, Andreas Pfadler, Ziniu Wu, and Jingren Zhou. 2023. Lero: A Learning-to-Rank Query Optimizer. Proceedings of the VLDB Endowment 16, 6 (Feb. 2023), 1466–1479. <https://doi.org/10.14778/3583140.3583160>